Atom-Atom Entanglement by Single-Photon Detection

L. Slodička,[1] G. Hétet,[1] N. Röck,[1] P. Schindler,[1] M. Hennrich,[1] and R. Blatt[1,2]

[1]*Institut für Experimentalphysik, Universität Innsbruck, Technikerstraße 25, 6020 Innsbruck, Austria*

[2]*Institut für Quantenoptik und Quanteninformation der Österreichischen Akademie der Wissenschaften, Technikerstraße 21a, 6020 Innsbruck, Austria*

(Received 23 July 2012; published 21 February 2013)

A scheme for entangling distant atoms is realized, as proposed in the seminal paper by [C. Cabrillo *et al.*, Phys. Rev. A **59**, 1025 (1999)]. The protocol is based on quantum interference and detection of a single photon scattered from two effectively one meter distant laser cooled and trapped atomic ions. The detection of a single photon heralds entanglement of two internal states of the trapped ions with high rate and with a fidelity limited mostly by atomic motion. Control of the entangled state phase is demonstrated by changing the path length of the single-photon interferometer.

DOI: 10.1103/PhysRevLett.110.083603 PACS numbers: 42.50.Ct, 32.80.Qk, 37.10.Rs

The generation of entanglement between distant physical systems is an essential primitive for quantum communication networks [1,2] and further tests of quantum mechanics. The realization of heralded entanglement between distant atomic ensembles [3,4] was amongst the first major achievements in this direction. Probabilistic generation of heralded entanglement between single atoms [5] was demonstrated using single trapped ions [6] and neutral atoms [7] with an entanglement generation rate given by the probability of coincident detection of the two photons coming from the atoms [8,9]. More recently, single neutral atoms trapped at distant locations were entangled by first generating the single atom-photon entanglement and then mapping the photonic state on the electronic state of the second atom [10]. A heralding mechanism will however be essential for efficient entanglement and scalability of quantum networks using realistic channels [2], and single qubit operations are required for distributed quantum information processing schemes [11]. In this Letter we report on the realization of a fundamental process which fulfills both these conditions by showing entanglement between two well-defined atomic qubits via emission and detection of a single light quantum [12]. In this scheme, both the energy and the phase of the emitted single photon are used for entanglement generation. In addition, this mechanism allows the demonstration of a large speedup in entanglement generation rate compared to the previously realized heralded entanglement protocol with single atoms [6,8]. This result will enable the practical distribution of quantum information over long distances using single atom architectures.

Entanglement of distant single atoms through the detection of a single photon, as proposed in the seminal work of Cabrillo *et al.* [12], is both a fundamental and a promising technique for the field of quantum information. The interconnection between quantum nodes based on this scheme would provide efficient distribution of quantum information in large scale quantum networks [8,9]. To generate heralded entanglement, two atoms (A, B) are both prepared in the same long-lived electronic state $|gg\rangle$. Each atom is excited with a small probability p_e to another metastable state $|e\rangle$ through a spontaneous Raman process ($|g\rangle \rightarrow |i\rangle \rightarrow |e\rangle$) by weak excitation of the $|g\rangle \rightarrow |i\rangle$ transition and spontaneous emission of the single photon on the $|i\rangle \rightarrow |e\rangle$. Here $|i\rangle$ denotes an auxiliary atomic state with a short lifetime. This Raman process entangles each of the atom's internal states with the emitted photon number, so the state of each atom and its corresponding light mode can be written as $\sqrt{1-p_e}|g,0\rangle e^{i\phi_L} + \sqrt{p_e}|e,1\rangle e^{i\phi_D}$. Here, the phases ϕ_L and ϕ_D correspond to the phase of the exciting laser at the position of atom A and the phase acquired by the spontaneously emitted photon on its way to the detector, respectively. Indistinguishability of the photons from the two atoms is achieved by overlapping their corresponding modes, for example using a beam splitter. The total state of the system consisting of both atoms and the light modes is then $(1-p_e)e^{i(\phi_{L,A}+\phi_{L,B})}|gg,0\rangle + \sqrt{p_e(1-p_e)}(e^{i(\phi_{L,A}+\phi_{D,B})}|eg,1\rangle + e^{i(\phi_{L,B}+\phi_{D,A})}|ge,1\rangle) + p_e e^{i(\phi_{D,A}+\phi_{D,B})}|ee,2\rangle$. Single photon detection projects the two-atom state onto an entangled state $|\Psi^\phi\rangle = \frac{1}{\sqrt{2}}(|eg\rangle + e^{i\phi}|ge\rangle)$. Since at least one atom must be excited, the probability of measuring such a state is then 1-p_e^2. Here p_e^2 is the probability of simultaneous excitation of both atoms. The absolute success probability of the entangled state generation in one experimental run is then $P_{\mathrm{succ}} = 2p_e(1-p_e)\eta$, where η is the overall detection efficiency of the generated photons. The phase of the generated entangled state ϕ corresponds to the sum of the phase difference acquired by exciting beam at the position of the two atoms and the phase difference acquired by the photons from the respective atoms upon travelling to the detector. The only limiting factor here is the probability of simultaneous excitation of the two atoms p_e^2, which can be, in principle, made arbitrarily small.

To experimentally demonstrate the creation of such a single-photon heralded entanglement two barium ions are trapped and cooled in a linear Paul trap [13]. As shown in Figs. 1(a) and 1(b), laser light at 493 nm is used to Doppler cool the ions and to detect their electronic states by means of electron shelving, and a laser field at 650 nm repumps the atoms to the $P_{1/2}$ level from the metastable $D_{3/2}$ state. By carefully adjusting the cooling and trapping parameters, the ions are always well within the Lamb-Dicke limit so that the photon recoil during the Raman scattering process is mostly carried by the trap. This ensures that only minimal information is retained in the motion of the ion about which atom scattered the photon during the entanglement generation process. The fluorescence photons are efficiently collected by two high numerical aperture lenses (NA ≈ 0.4) placed 14 mm away from the atoms. A magnetic field of 0.4 mT is applied at an angle of 45 degrees with respect to the two-ion axis and defines the quantization axis. After passing through a polarizing beam splitter that blocks the π-polarized light and lets σ-polarized light pass, the spatial overlap of the photons is guaranteed by collecting the atomic fluorescence of the first ion in a single mode optical fiber, whilst the fluorescence of the second ion is sent to a distant mirror that retroreflects it in the same optical fiber [15]. The fluorescence of the two ions (including the Raman scattered light) is then detected by an avalanche photodiode with a quantum efficiency of 60%.

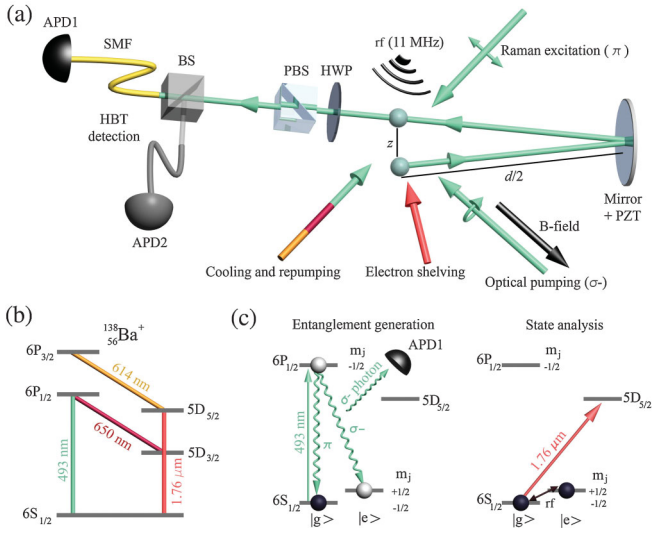

FIG. 1 (color). Experimental procedure for entanglement generation. (a) The fluorescence of the two ions is overlapped using a distant mirror which sets the effective distance between them to $d = 1$ meter. A half wave plate (HWP), a polarizing beam splitter (PBS), single-mode fiber (SMF), beam splitter (BS), piezoelectric transducer (PZT) and a single-mode optical fiber select the polarization and the spatial mode before an avalanche photodiode (APD1). A nonpolarizing beam splitter and an additional avalanche photodiode (APD2) can be inserted to form a Hanbury Brown–Twiss setup. See details in main text. (b) Level scheme of $^{138}Ba^{+}$ including the wavelengths of the lasers used in our experiment. (c) Experimental sequence. Spontaneous Raman scattering to $|e\rangle$ triggers emission of a single photon from the two atoms. Upon successful detection of a σ^{-} photon, state analysis comprising coherent radio-frequency (rf) pulses at 11 MHz, and electron shelving to the $5D_{5/2}$ level are performed. See details in main text.

For efficient generation of the two-atom entangled state, the emitted photons must be indistinguishable in all degrees of freedom at the position of the triggering detector. We characterize their indistinguishability by a measurement of the first and second order correlation functions (see Supplemental Material A [14]). These measurements yield unambiguous separation between the major decoherence mechanisms and lead to the conclusion that which-way information given by atomic motion is the main source of distinguishability.

In the entanglement generation procedure, we first Doppler cool the ions and stabilize the mirror-ion distance $d/2$ by locking the position of the interference fringe measured during the Doppler cooling sequence to a chosen position, see Fig. 1(a). The ion internal states are then prepared to the Zeeman substates $|6S_{1/2}, m_j = -1/2\rangle = |g\rangle$ by optical pumping with a circularly polarized laser pulse propagating along the magnetic field. Then, a weak horizontally polarized laser pulse (Raman excitation) excites both ions on the $S_{1/2} \leftrightarrow P_{1/2}$ transition with a probability $p_e = 0.07$ through a resonant spontaneous Raman scattering to the other Zeeman sublevel ($m_j = +1/2$) of the $6S_{1/2}$ state, $|e\rangle$. The electronic state of each ion is at this point entangled with the number of photons $|0\rangle$ or $|1\rangle$ in the σ^{-} polarized photonic mode. Provided that high indistinguishability of the two photonic channels is assured and that simultaneous excitation of both atoms is negligible, detection of a single σ^{-} photon on the avalanche photodiode (APD) projects the two-ion state onto the maximally entangled state $|\Psi\rangle = \frac{1}{\sqrt{2}}(|ge\rangle + |eg\rangle e^{ikd})$, where k is the wave number of the 493 nm fluorescence. The phase factor e^{ikd} corresponds here solely to the phase difference $\phi_{D,A} - \phi_{D,B}$ acquired by the emitted photon upon its way to the detector. The phase difference of the excitation laser at the position of two ions $\phi_{L,A} - \phi_{L,B}$ is fixed to $n \times 2\pi$, $n \in I$ by setting the mutual distance between the ions in the trap to $z = n\lambda/\cos\theta$, where θ is the angle between the Raman-excitation laser direction and the ion-crystal axis. We will first demonstrate a successful preparation of the Bell state $|\Psi^{+}\rangle$ for the phase $e^{ikd} = 1$ corresponding to an antinode of the interference fringe.

Following the detection of a Raman scattered σ^{-} photon, we coherently manipulate the generated two-atom state to allow for measurements in different bases. As shown in Fig. 1(c), this is done by first applying radio-frequency (rf) pulses that are resonant with the $|g\rangle \leftrightarrow |e\rangle$ transition of both atoms. Discrimination between the two Zeeman sublevels of the $S_{1/2}$ state is finally done by

shelving the population of the $m_j = -1/2$ state to the metastable $D_{5/2}$ level using a narrow band 1.76 μm laser [13]. The fluorescence on the $S_{1/2} \leftrightarrow P_{1/2}$ transition allows us to measure the two-atom state. By setting the appropriate thresholds on the fluorescence counting histogram, we can discriminate the three possible cases where no excitations are present in the two atoms, a single excitation is shared between the two atoms, and where two atoms are excited. These events can all be separated with 98% probability, enabling us to efficiently reconstruct the relevant parts of the density matrix of the two-atom state. The 614 nm laser field then resets the ions to the $6S_{1/2}$ state and the same experiment is repeated 100 times.

Figure 2(a) shows the measurement results obtained without the rf analysis pulses. The results tell us that

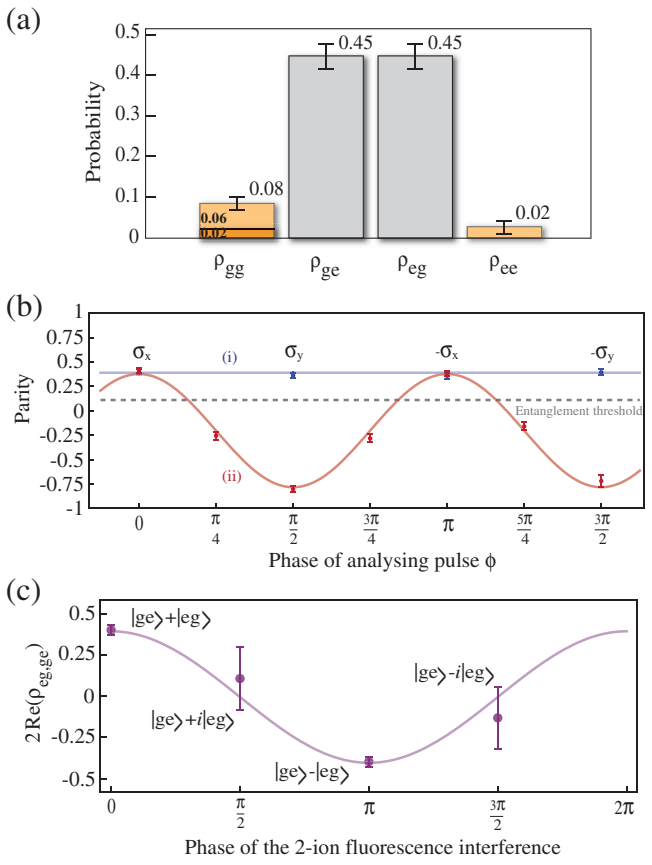

FIG. 2 (color). Characterization of the entangled state. (a) Two-atom state populations after the detection of a σ^- photon showing that the total probability of measuring the state with a single excitation is 90%. (b) Parity measurements as a function of the rf phase. Trace (ii) corresponds to the measurement of the atomic populations after two global rotations $\hat{R}^g(\pi/2, \phi)\hat{R}^g(\pi/2, \pi/2)$. In the measurement of trace (i) only a single global rf pulse $\hat{R}^g(\pi/2, \phi)$ is applied. The dashed line shows the threshold for entanglement, estimated from the measured diagonal terms. (c) Real part of the coherence between the $|ge\rangle$ and $|eg\rangle$ states as a function of the phase of the optical path difference between the two ions.

$89 \pm 3\%$ of all the triggering events signal that only one of the atoms was excited to the $|e\rangle$ state. The remaining 10% errors are caused by APD dark counts and double excitation of the ions. Our detection process using a single photomultiplier doesn't allow us to resolve individual ρ_{eg} and ρ_{ge} populations directly, but it tells us the number of the excited atoms, and so, the sum of these terms. Although individual populations of the ρ_{eg} and ρ_{ge} states are not needed for estimation of the fidelity with the state $|\Psi^+\rangle$, we also experimentally prove that ρ_{eg} and ρ_{ge} populations are approximately the same and depend only on the overall fluorescence detection efficiencies from the two ions. In order to measure the quantum coherence of the generated state, we then apply two consecutive global rf pulses, each corresponding to the rotation $\hat{R}(\theta, \phi) = \exp[-i\frac{\theta}{2}(\cos\phi\hat{S}_x + \sin\phi\hat{S}_y)]$, where $\hat{S}_{x,y} = \hat{\sigma}^{(1)}_{x,y} \otimes \hat{\sigma}^{(2)}_{x,y}$ is the global Pauli operator acting on both ions. The rotation angle θ and rotation axis ϕ on the Bloch sphere are determined by the duration and the phase of the rf pulses, respectively. We first apply the pulse $\hat{R}(\pi/2, \pi/2)$ which performs the unitary rotation $\hat{R}(\pi/2, \pi/2)|\Psi^+\rangle \rightarrow |\Phi^-\rangle$, where $|\Phi^-\rangle = \frac{1}{\sqrt{2}}(|gg\rangle - |ee\rangle)$. A second rf pulse with the same duration, but with a phase ϕ, then performs the rotation $\hat{R}(\pi/2, \phi)|\Phi^-\rangle$. After shelving the state $|e\rangle$ to the metastable level $D_{5/2}$, we scatter light from both ions on the cooling transition. From the measured fluorescence rate at different phases ϕ, we extract the mean value of the parity operator defined as $\hat{P} = \hat{p}_{gg} + \hat{p}_{ee} - \hat{p}_{eg} - \hat{p}_{ge}$, where $\hat{p}_{ij}$ are the projection operators on states $|ij\rangle$, $i, j \in \{g, e\}$ [16] (see Supplemental Material B [14]).

Figure 2(b), trace (ii), shows the results of the parity operator measurements preceded by two global rf rotations $\hat{R}(\pi/2, \phi)\hat{R}(\pi/2, \pi/2)$. The measured parity clearly oscillates as a function of phase ϕ with contrast of $58.0 \pm 2.5\%$ and a period of π, a proof that we indeed succeed in preparing an entangled two-ion state close to $|\Psi^+\rangle$ [16]. The mean value of the parity operator at zero phase $\langle\hat{P}\rangle_{\phi\rightarrow 0}$ corresponds to the difference between the inner parts and outermost coherence terms of the density matrix. We evaluate it to be $2\,\mathrm{Re}(\rho_{\mathrm{ge,eg}} - \rho_{\mathrm{gg,ee}}) = 0.38 \pm 0.03$. To precisely quantify the fidelity of our state with $|\Psi^+\rangle$, we however need to estimate the real part of the coherence $\rho_{ge,eg}$ itself. This is done by measuring the parity without the first rf rotation. Trace (i) of Fig. 2(b) shows the expectation value of the parity as a function of the phase ϕ of the single rf pulse $\hat{R}(\pi/2, \phi)$. The only oscillatory term contributing to this parity measurement reads $2[\sin(2\phi)\mathrm{Im}\rho_{\mathrm{gg,ee}} - \cos(2\phi)\mathrm{Re}\rho_{\mathrm{gg,ee}}]$. The measured data, however, shows the independence of the parity signal with respect to the phase ϕ within the measurement error. Therefore, only the coherence corresponding to the state $|\Psi^+\rangle$ contributes to the parity signal (ii). The value of the coherence $\mathrm{Re}(\rho_{gg,ee})$ estimated from these measurements

is $\mathrm{Re}(\rho_{gg,ee}) = 0.00 \pm 0.03$. We finally estimate that the fidelity of the generated state with the maximally entangled state $|\Psi^+\rangle$ is $F = 64 \pm 2\%$. The threshold for an entanglement is thus surpassed by more than six standard deviations.

The coherence between the $|ge\rangle$ and $|eg\rangle$ states of $38 \pm 3\%$ is limited by three main processes. First, imperfect populations of $|ge\rangle$ and $|eg\rangle$ states set a limit of 89% [17]. Around 4% of the coherence loss can be attributed to the finite coherence time of the individual atomic qubits (120 μs) due to collective magnetic field fluctuations. Although the generated $|\Psi^+\rangle$ state is intrinsically insensitive against collective dephasing [18,19], a loss of coherence is indeed expected after the rotation of $|\Psi^+\rangle$ out of the decoherence-free subspace. The highest contribution to the coherence loss can be attributed to atomic motion, which can provide information about which atom emitted the photon. Around 55% of the coherence is lost due to the atomic recoil kicks during the Raman scattering (see Supplemental Material C [14]). Error bars in the presented measurements results correspond to one standard deviation and are estimated statistically from several experimental runs each giving approximately 120 measurement outcomes. Up to 60% of the measurement error is caused by the quantum projection noise. Additional uncertainty comes from slow magnetic field drifts with a magnitude of several tens of nT making the rf driving off-resonant by tens of kHz.

An intrinsic feature of the realized entangling protocol is the dependence of the generated entangled state phase on the optical path difference between the ions. To demonstrate this, we measure the real part of the coherence between the $|ge\rangle$ and $|eg\rangle$ states as a function of the phase factor kd. Figure 2(c) reveals a large change of the real part of the coherence from positive to negative values when going from the maximum to the minimum of the interference signal, in agreement with the e^{ikd} phase dependence of the entangled state.

An important feature of the single-photon heralding mechanism is the high entanglement generation rate that can be achieved. With our experimental setup, the single photon detection scheme indeed yields a higher rate compared to the two photon scheme proposed by Simon *et al.* [5,7,8,20]. The probability of preparing an entangled state depends on the probability of the single photon detection and the Raman scattering probabilities [8], which in our case gives a total of $P_{\mathrm{succ}} = 1.1 \times 10^{-4}$ for each trial run. With an experimental duty cycle of 2.3 kHz, this corresponds to 15.4 successful entanglement generation events/minute, which is in good agreement with the experimentally observed 14 ± 2 events/minute. A detailed analysis of the overall photon-detection efficiency can be found in the Supplemental Material E [14].

We have demonstrated a fundamentally new protocol for generating heralded entanglement between two ions. This was achieved via the scheme proposed in the seminal work of Cabrillo *et al.* [12], where two atoms are entangled with the emission and detection of only one photon. Such a single-photon scheme allowed us to reach a rate of entanglement generation of 14 events/minute, more than two orders of magnitude higher than the rate obtainable with protocols relying on a two-photon coincidence event with our experimental parameters. The maximally entangled state $|\Psi^+\rangle$ is produced with a fidelity of 63.5% limited mostly by residual atomic motion. These results can be improved by cooling all of the involved motional modes close to their ground state [13] or choosing a different excitation direction to minimize residual which-way information. These improvements, together with the experimental results presented, will enable efficient creation and distribution of entanglement between distant sites with well-defined and controllable atomic qubits. Such entanglement generation corresponds to an essential building block of scalable quantum communication [11] and distributed quantum computation [21–23] architectures with single atoms.

We thank J. Eschner, T. Monz, T. Northup, and A. Stute for helpful discussions. This work was supported by the Austrian Science Fund (FWF), the Institut für Quanteninformation GmbH, and a Marie Curie International Incoming Fellowship within the 8th European Framework Program.

[1] H.-J. Briegel, W. Dür, J. I. Cirac, and P. Zoller, Phys. Rev. Lett. **81**, 5932 (1998).
[2] L. M. Duan, M. D. Lukin, J. I. Cirac, and P. Zoller, Nature (London) **414**, 413 (2001).
[3] C. W. Chou, H. de Riedmatten, D. Felinto, S. V. Polyakov, S. J. van Enk, and H. J. Kimble, Nature (London) **438**, 828 (2005).
[4] C. W. Chou, J. Laurat, H. Deng, K. S. Choi, H. de Riedmatten, D. Felinto, and H. J. Kimble, Science **316**, 1316 (2007).
[5] C. Simon and W. T. M. Irvine, Phys. Rev. Lett. **91**, 110405 (2003).
[6] D. L. Moehring, P. Maunz, S. Olmschenk, K. C. Younge, D. N. Matsukevich, L.-M. Duan, and C. Monroe, Nature (London) **449**, 68 (2007).
[7] J. Hofmann, M. Krug, N. Ortegel, L. Gerard, M. Weber, W. Rosenfeld, and H. Weinfurter, Science **337**, 72 (2012).
[8] S. Zippilli, G. A. Olivares-Rentería, G. Morigi, C. Schuck, F. Rohde, and J. Eschner, New J. Phys. **10**, 103003 (2008).
[9] L. Luo, D. Hayes, T. A. Manning, D. N. Matsukevich, P. Maunz, S. Olmschenk, J. D. Sterk, and C. Monroe, Fortschr. Phys. **57**, 1133 (2009).
[10] S. Ritter, C. Nölleke, C. Hahn, A. Reiserer, A. Neuzner, M. Uphoff, M. Mücke, E. Figueroa, J. Bochmann, and G. Rempe, Nature (London) **484**, 195 (2012).
[11] L.-M. Duan and C. Monroe, Rev. Mod. Phys. **82**, 1209 (2010).

[12] C. Cabrillo, J. I. Cirac, P. Garcia-Fernández, and P. Zoller, Phys. Rev. A **59**, 1025 (1999).
[13] L. Slodička, G. Hétet, N. Röck, S. Gerber, P. Schindler, M. Kumph, M. Hennrich, and R. Blatt, Phys. Rev. A **85**, 043401 (2012).
[14] See Supplemental Material http://link.aps.org/supplemental/10.1103/PhysRevLett.110.083603 for details of measurements of photon indistinguishability (parts A and D), description of parity measurements (B), analysis of the quantum coherence of generated state (C), and the generation process efficiency (E).
[15] We note that in our setup, super-/subradiance effects that might occur here are on the order of 1%, and can thus be neglected. See S. Rist, J. Eschner, M. Hennrich, and G. Morigi, Phys. Rev. A **78**, 013808 (2008).
[16] C. A. Sackett *et al.*, Nature (London) **404**, 256 (2000).
[17] M. Shirokov, Int. J. Theor. Phys. **45**, 141 (2006).
[18] C. F. Roos, G. P. T. Lancaster, M. Riebe, H. Häffner, W. Hänsel, S. Gulde, C. Becher, J. Eschner, F. Schmidt-Kaler, and R. Blatt, Phys. Rev. Lett. **92**, 220402 (2004).
[19] D. Kielpinski, V. Meyer, M. A. Rowe, C. A. Sackett, W. M. Itano, C. Monroe, and D. J. Wineland, Science **291**, 1013 (2001).
[20] D. N. Matsukevich, P. Maunz, D. L. Moehring, S. Olmschenk, and C. Monroe, Phys. Rev. Lett. **100**, 150404 (2008).
[21] L. Jiang, J. M. Taylor, A. S. Sørensen, and M. D. Lukin Phys. Rev. A **76**, 062323 (2007).
[22] J. I. Cirac, A. K. Ekert, S. F. Huelga, and C. Macchiavello Phys. Rev. A **59**, 4249 (1999).
[23] D. Gottesman and I. L. Chuang, Nature (London) **402**, 390 (1999).